

Design & Performance of A Compact Helical Counterflow Heat Exchanger

K.Ramesh¹, K.Durga Prasad²

¹M.Tech student, V.K.R, V.N.B & A.G.K College of Engineering, Gudivada

²Asst.Prof, V.K.R, V.N.B & A.G.K College of Engineering, Gudivada

Abstract-Compact heat exchangers are desirable in many aerospace applications. New additive manufacturing approaches, such as 3D printing, have enabled the fabrication of heat exchange devices utilizing geometries that cannot be fabricated using traditional approaches. The new geometries enabled by 3D printing may result in higher heat transfer using smaller devices; however, constraints associated with the fabrication of these devices also impose potential performance degradations. This work presents the design and analysis of a novel, compact counter flow heat exchanger which uses helically shaped passages to enhance the effectiveness of the heat transfer and reduce the size of the device, 3D print build constraints mandate that the passages are constructed with a lean angle for structural support that also increases the overall pressure loss of the fluid. An analytical model is developed, that can be used to trade the size and mass of the device for required heat transfer performance and acceptable levels of fluid pressure loss. Various working fluids, including water and cryogenics are considered and designs that meet specified heat transfer goals while minimizing the pressure loss and volume of the device are presented. These designs are compared against a straight channel counter flow heat exchanger which can be fabricated using traditional approaches. This work demonstrates that for the same working fluids and for a set of given geometric constraints a tradeoff between heat exchange, pressure loss and compactness is observed while designing an optimized model.

I. BACKGROUND

Heat Exchangers are one of the most important components in many industrial processes and cover a wide range of industrial applications. Heat exchangers have been used in power plant, electronics, environmental engineering, manufacturing industry, air-conditioning, waste heat recovery, cryogenic processes, chemical processing steam power plants, transportation power systems, refrigeration units. Heat exchangers have come long way, from large ones transported in trucks, airplanes to small ones which can fit in the palm of our hands. Factors like cost of fabrication and installation, weight and size play important roles in choosing an appropriate design. Heat exchangers can be classified according to transfer process, construction, number of fluids, surface compactness, flow arrangement and heat transfer mechanisms.

1.2 Objectives

The objectives of this thesis are to:

- 1) Develop an analytical model that can be used to optimize the design of a 3D printed, compact counter-flow heat exchanger.
- 2) Identify relevant performance metrics, including heat exchange, working fluid pressure drop, compactness, cost, manufacturability, etc.
- 3) Use the model to assess the performance of a new compact counter-flow heat exchanger design over a range of relevant fluids, flow conditions and targeted heat exchange.
- 4) Assess a variety of geometric configurations for important performance metrics, including heat exchanger, pressure loss, volume, mass, manufacturability, etc.
- 5) Optimize design for range of flow condition and based on a set of constraints.

II. COUNTERFLOW HEAT EXCHANGER ANALYSIS OVERVIEW

Cylindrical, annular counter low heat exchangers have been extensively investigated and are discussed in literature. This section presents an overview of a special class of cylindrical, annular counterflow heat exchangers, which is used in many engineering applications where the central region of the heat exchanger is left open for several reasons, such as locating other internal components, and because locating the flow passages further radially outward increases surface area available for heat exchange. This type of heat exchanger is shown in Figure 2.1.

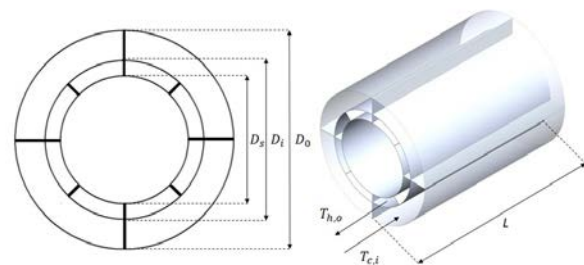


Figure 2.1: Cylindrical Annular Straight Counter flow Heat Exchanger

The heat exchanger shown in Figure 1 has two concentric annular channels. In this figure, the outer annular channel has 4 fins and thus 4 passages and the inner has 8 passages. The diameters shown in Figure 1 are centerline diameters, meaning that the diameters are those to the center of the

walls. The outer diameter is D_o , the inner diameter is D_i and the innermost is D_s . The wall thickness of the outer, t_o , inner, t_i , innermost, t_s and fin thickness, t_f are included in the geometric calculations however, the walls present no thermal resistance. Based on the thickness of the channel walls and the diameters the heights of the individual channels can be determined. For example, the outer channel height is $D_o - t_o - (D_i + t_i)$. The length of the heat exchanger is denoted by L .

The important parameters for the heat exchanger are the inlet temperatures, pressures, and mass flow of the two working fluids, and the geometry of the device. For this device, and in the analyses, that follow, hot fluid flows in the inner channels and the cold fluid flows in the outer channel. The fluids always flow counter to each other.

The analyses assume that the heat exchanger operates in steady-state, is adiabatic, and that the flows enter the heat exchanger fully developed in both momentum and thermal profiles. Energy balance equations are used to find the required overall heat transfer coefficient. Equation (1) and (2) give the energy balance for the hot and cold fluid, respectively.

$$q = \dot{m}_h (h_{h,o} - h_{h,i}) \quad (1)$$

$$q = \dot{m}_c (h_{c,i} - h_{c,o}) \quad (2)$$

Where q is the heat transfer rate from either hot to cold fluid or from cold to hot fluid, \dot{m}_h is the mass flow rate of hot fluid, $h_{h,i}$ is the inlet enthalpy of the hot fluid, $h_{h,o}$ is the outlet enthalpy of the hot fluid, \dot{m}_c is the mass flow rate of cold fluid, $h_{c,i}$ is the inlet enthalpy of the cold fluid, and $h_{c,o}$ is the outlet enthalpy of the cold fluid. For example, with known mass flow rates, inlet temperatures, and the desired exit temperature of one of the other fluids, the heat transfer rate and exit temperature of the other fluid can be found.

Equation (3) gives the heat transfer rate from the hot fluid to the cold fluid or vice-versa in the heat exchanger

$$q = U_{req} A_s \Delta T_{lm}$$

A_s is the heat transfer surface area, U_{req} is the overall heat transfer coefficient that is required to achieve the desired heat exchange, and ΔT_{lm} is the log means temperature difference of the fluids, given by Equation (4).

$$\Delta T_{lm} = \frac{\Delta T_1 - \Delta T_2}{\ln(\Delta T_1 / \Delta T_2)} \quad (4)$$

$$\Delta T_1 = T_{h,i} - T_{c,o} \quad (5)$$

$$\Delta T_2 = T_{h,o} - T_{c,i} \quad (6)$$

Where ΔT_1 and ΔT_2 are the temperature differences of the fluid temperatures at the inlet and outlet of the heat exchanger channels, $T_{h,i}$ and $T_{h,o}$ are the temperatures of

the hot fluid at inlet and exit respectively. Likewise, $T_{c,i}$ and $T_{c,o}$ are the temperatures of the cold fluid at inlet and exit respectively.

The achievable overall heat transfer coefficient is the inverse of the total thermal resistance between two fluids. Generally, the coefficient is determined by accounting for conduction and convection resistances between fluids separated by composite plane and cylindrical walls respectively. In this analysis, zero wall resistance is assumed and thus the achievable overall heat transfer coefficient is determined from the hot and cold fluid convection coefficients and from appropriate geometric parameters. Equation (7) gives the expression for achievable overall heat transfer coefficient.

$$U_{ach} = \left(\frac{1}{h_h} + \frac{1}{h_c} \right)^{-1} \quad (7)$$

In this expression h_h and h_c are the hot and cold convective coefficients respectively. The convective heat transfer coefficient is found using equation (8):

$$h = Nu \frac{k}{D_h} \quad (8)$$

In equation (6), Nu is the Nusselt number, k is the thermal conductivity of the fluid and D_h is the hydraulic diameter and is given by Equation (9):

$$D_h = \frac{4A_{crs}}{p} \quad (9)$$

In the above equation A_{crs} is the cross-sectional area and p is the wetted perimeter. Nusselt number is a function of the two dimensionless quantities, Reynolds, Re_D and Prandtl, Pr number. Reynolds and Prandtl number is given by equation (10) and (12) respectively.

$$Re_D = \frac{\rho v D_h}{\mu} \quad (10)$$

$$v = \frac{\dot{m}}{\rho A_{crs}} \quad (11)$$

$$Pr = \frac{c_p \mu}{k} \quad (12)$$

In the above equations ρ, C_p, μ are the density, Specific heat at constant pressure and viscosity of the fluid respectively and v is the fluid velocity. Therefore, convective heat transfer depends on the flow regime, fluid properties, geometry and convective heat transfer coefficients are analyzed for two different counterflow heat exchanger design/model, a straight and a helical annular heat exchanger.

The fluid pressure drop is an important parameter in heat exchanger analysis and minimizing is always favorable. The frictional pressure drop, ΔP along the length of the channel is given by Equation (13):

$$\Delta p = \frac{fL\dot{m}}{2\rho D_h A_{crs}^2} \dots \dots \dots (13)$$

Where f is the frictional factor, L is the length of the channel, \dot{m} is the mass flow rate of the fluid, ρ is the density of the fluid, D_h is the hydraulic diameter of the pipe and A_{crs} is the cross-sectional area of the channel. The frictional factor correlations for different types of heat exchangers are discussed in the next section.

III. COUNTERFLOW HEAT EXCHANGER ANALYTICAL MODELING

This section develops analytical models for several types of counterflow heat exchangers in order to trade relevant device performance parameters such as overall heat transfer rates, resulting flow temperatures, pressure loss, as well as the physical characteristics of the device such as volume and mass. This work develops an analytical model which determines the heat transfer performance and pressure drop for a heat exchanger design and then the design is optimized to increase heat transfer performance and decrease pressure drop. Three geometric categories of counterflow heat exchanger are considered: subsection 3.1 examines cylindrical, annular geometries without and with radial fins, subsection 3.2 develops a model for a cylindrical, annular heat exchanger in which the flow passages are helically wrapped around the device, and subsection 3.3 extends the models in subsection 3.2 to include a lean angle of the radial fins that is required for the fabrication of a such a device using additive manufacturing.

3.1. Straight Annular Heat Exchanger without and with Radial Fins

This section describes the analytical modeling for a counterflow heat exchanger where both the cold flow and the hot flow passages are straight – meaning that the passages are parallel to the central axis of the heat exchanger and the flows move parallel to the central axis of the heat exchanger, as shown in Figure 1. Radial elements can be added which divides both the cold and the hot passages into individual channels. The radial elements act as fins to promote greater heat transfer and act as flow straighteners which keep the flows moving parallel to the axial direction of the heat exchanger. The penalty associated with adding these radial elements is that there is more flow-surface interaction, typically resulting in larger pressures losses of the working fluids. A schematic of a straight counter flow heat exchanger with 4 channels in the cold section and 8 channels in the hot section was shown in Figure 2-1. The cross-sectional area and the perimeter for passage as shown in figure 2-1 is calculated appropriately by taking diameter, wall and fin thickness into account. For example, the cross-sectional area and perimeter of a passage in the outer channel is given by equation (14) and (15).

$$A_{crs} = \frac{1}{n} \left(\frac{\pi(D_o - t_o)^2}{4} - \frac{\pi(D_i + t_i)^2}{4} \right) - \left(\frac{t_i - t_o}{2} + D_o - D_i \right) t_f \dots \dots \dots (14)$$

$$p = \frac{1}{n} \left(\pi \left(D_o + D_i + \frac{t_i - t_o}{2} \right) \right) + 2 \left(D_o - D_i - \frac{t_o + t_i}{2} \right) - t_f \dots \dots \dots (15)$$

Nusselt number is a function of Reynolds number and Prandtl number and equation (16) and (17) gives the Nusselt number correlations which are valid for straight channels.

$$Nu_D = 4.36 \dots \dots \dots (16)$$

$$Nu_D = \frac{(f/8)(Re_D - 1000)Pr}{1 + 1.27(f/8)^{0.5} (Pr^{2/3} - 1)} \dots \dots \dots (17)$$

$$f = (0.790 \ln Re_D - 1.64)^{-2} \dots \dots \dots (18)$$

The flow is assumed to be fully developed and is under a uniform heat flux. Equation (16) is used when the flow is laminar and $Pr \geq 0.6$. In the above expressions f is the Darcy frictional factor, Re_D is the Reynolds number (based on hydraulic diameter) and Pr is the Prandtl number. The correlation in equation (17) is valid for, $3,000 \leq Re_D \leq 5 \times 10^6$, $0.5 \leq Pr \leq 2,000$ and $L \geq 10D_h$. Based on the flow regime and Pr , an appropriate Nu correlation is chosen and the convective heat transfer coefficient is found for both the hot and cold fluids and ultimately the achievable overall heat transfer coefficient is found using equation (7).

The achievable overall heat transfer coefficient is given by equation (19) when fins are added. Fins increase the surface area exposed to heat transfer and they reduce the resistance to convective heat transfer and the overall fin efficiency is given by equation (20).

$$U_{ach} = \left(\frac{1}{(\eta_o h)_h} + \frac{1}{(\eta_o h)_c} \right)^{-1} \dots \dots \dots (19)$$

$$\eta_o = 1 - \frac{A_f}{A} (1 - \eta_f) \dots \dots \dots (20)$$

In the above expressions η_o is the overall fin efficiency, η_f is the efficiency of a single fin, A_f is the fin surface area and A is the total surface area. The efficiency of a fin is calculated using equation (21) and under the assumption that the tip of the fin is adiabatic.

$$\eta_f = \frac{\tanh(mL)}{mL} \dots \dots \dots (21)$$

$$m = \sqrt{\frac{2h}{k_f t_f}} \dots \dots \dots (22)$$

In the above expressions t_f is the fin thickness, h is the convective heat transfer coefficient of the fluid and k_f is the thermal conductivity of the fin. In case of straight pipes, the frictional factor for laminar flow regime is given by equation (23) and Colebrook-white equation is used for turbulent regime as shown in equation (24).

$$f_s = 64/Re_D \dots \dots \dots (23)$$

$$\frac{1}{\sqrt{f_s}} = -2\log_{10} \left[\frac{\epsilon/D_h}{3.7} - \frac{2.51}{Re_D \sqrt{f_s}} \right] \dots \dots \dots (24)$$

In the above equation f_s is the frictional factor for straight tubes and ϵ is the surface roughness of the pipe material.

3.2. Helical Annular Heat Exchanger with Radial Fins

This section presents a heat exchanger concept similar to that shown in Figure 2-1, however, the channels are now helical, rather than straight passages. A schematic of the helical annular counter flow heat exchanger concept with 8 channels in the cold (outer) section and 4 channels in the hot (inner) section is shown in Figure 3-1.

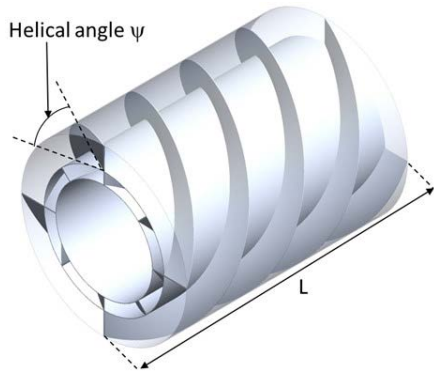


Figure 3-1: Cylindrical Helical Annular Counterflow Heat Exchanger with $N = 0.5$, $\Psi = 37.6^\circ$, $L_{hlx}/L = 1.26$ for inner channels and $N=1$, $\Psi = 26.2^\circ$, $L_{hlx}/L = 2.26$ for the outer channels.

The helical passages are characterized by the number of turns, N , over the length of the heat exchanger, L , or the helical angle, Ψ . The length of the helical channel, l_{hlx} , and helical angle, Ψ are given by Equations (25) and (26).

$$L_{hlx} = \sqrt{(2\pi Nr)^2 + L^2} \dots \dots \dots (25)$$

$$\Psi = \cos^{-1} \left(L/L_{hlx} \right) \dots \dots \dots (26)$$

In the above equations, N is the number of helical turns, r is the radiuses of helix i.e. distance from the center of the heat exchanger to the center of the channel and L is the length of the heat exchanger. In case of helical passages, the cross-sectional area and the wetted perimeter of a single passage is found by taking diameter, wall and fin thickness and helical angle, Ψ into account. For example, cross-sectional area and perimeter of a passage in the outer channel is given by equation (27) and (28).

$$A_{crs} = \left[\frac{1}{n} \left(\frac{\pi(D_o - t_o)^2}{4} - \frac{\pi(D_i + t_i)^2}{4} \right) - \left(\frac{t_i - t_o}{2} + D_o - D_i \right) t_f \right] \cos \Psi \dots \dots \dots (27)$$

$$P = \left[\frac{1}{n} \left(\pi \left(D_o + D_i + \frac{t_i - t_o}{2} \right) \right) \right] \cos \Psi + 2 \left(D_o - D_i - \frac{t_o + t_i}{2} \right) - 2t_f \dots \dots \dots (28)$$

The secondary flow within the passages is an important characteristic of the helical heat exchanger. The dimensionless Dean number, De , is used in the analysis in addition to those used in straight round channels and is given by Equation (29). The critical Reynolds number, is used to identify the transition from laminar to turbulent flow in curved or helical pipes, is calculated as shown in equation (30).

$$De = Re_D (a/R)^{1/2} \dots \dots \dots (29)$$

$$Re_{crit} = 2100 \left(1 + 12(R/a)^{-0.5} \right) \dots \dots \dots (30)$$

In the above expressions a denotes the radius of the helical channel. For helical coils, no single $Recrit$ exists because of the varying curvature. For helical coils with constant heat flux, the Nusselt number has been developed by Manlapaz and Churchill [20] for laminar fully developed flow and is given by equation (31). Nusselt correlations for turbulent flow developed by Schmidt [20] is suggested for $2 \times 10^4 < Re < 1.5 \times 10^5$ and $5 < Ra < 84$ and is given by equation (34). For low Reynolds number Pratt's correlation is recommended and is for $1.5 \times 10^3 < Re < 2 \times 10^4$ and is given by equation (35).

$$Nu_{cv} = \left[\left(4.364 + \frac{4.636}{X_3} \right)^3 + 1.816 \left(\frac{De}{X_4} \right)^{3/2} \right]^{1/3} \dots \dots \dots (31)$$

$$X_3 = \left(1 + \frac{1342}{De^2 pr} \right)^2 \dots \dots \dots (32)$$

$$X_4 = 1 + \frac{1.15}{pr} \dots \dots \dots (33) Nu_{cv}$$

$$= Nu_s \left[1 + 3.6 \left[\left(1 - \frac{a}{R} \right) \left(\frac{a}{R} \right)^{0.8} \right] \right] \dots \dots \dots (34)$$

$$Nu_{cv} = Nu_s \left[1 + 3.4 \left(\frac{a}{R} \right) \right] \dots \dots \dots (35)$$

In the above expressions, Nu_{cv} is the Nusselt number for curved or helical pipes and Nu_s is the Nusselt number for straight pipes. In helical coils, the flow generally becomes fully developed within the first half turn of the coil. The required and achievable convective heat transfer coefficient is calculated using equation (7) and (19). Frictional factor for a fully developed laminar flow in helical coil proposed by Manlapaz and Churchill [21] is given by equation (36)

$$\frac{f_{cv}}{f_s} = \left[\left(1 - \frac{0.18}{[1+(35/De)^2]^{0.5}} \right)^m + \left(1 + \frac{a/R}{3} \right)^2 \left(\frac{De}{88.33} \right)^{0.5} \right] \dots \dots \dots (36)$$

In the above equation f_c is the frictional factor for curved pipes, f_s is the frictional factor for straight pipes, $m = 2$ for $De < 20$; $m = 1$ for $20 < De < 40$; and $m = 0$ for $De > 40$. Appropriate f_s can calculate based on Re_D and from the correlations given by equation (23) and (24). Turbulent flow frictional factors as shown in equation (37) was developed by Srinivasan and can be used when $Re \left(\frac{R}{a} \right)^{-2} < 700$ and $7 < \frac{R}{a} < 104$.

$$f_{cv} \left(\frac{R}{a} \right)^{0.5} = 0.084 \left[Re \left(\frac{R}{a} \right)^{-2} \right]^{-0.2} \dots \dots \dots (37)$$

3.3. Helical Annular Heat Exchanger with Radial Fins and Lean

The geometry shown in Figure 3-1 represents a highly compact and efficient device, however, the geometry cannot be fabricated using 3D printing because there is no way to build-up the helical passage walls due to them being cantilevered perpendicular from the wall without support. To amend this issue, a lean angle is used during the build. A schematic of the heat exchanger with 8 channels in the cold section and 4 channels in the hot section with fins having a lean angle is shown in Figure 3-2.

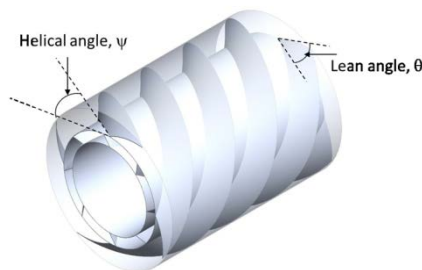


Figure 3-2 : Cylindrical Helical Annular Counterflow Heat Exchanger with $N = 0.5$, $\Psi = 37.6^\circ$, $L_{htx}/L = 1.26$ for inner channels and $N=1$,

$\Psi = 26.2^\circ$, $L_{htx}/L = 2.26$ for the outer channels with $\theta = 45^\circ$ in both the channels

In case of radial fins with a lean angle, θ the area of the passage remains the same, but the wetted perimeter changes when compared to those of the model without lean and is shown by equation (38).

$$p = \left[\frac{1}{n_o} \left(\pi \left(D_o + D_i + \frac{t_i - t_o}{2} \right) \right) \right] \cos \Psi + 2 \left(D_o - D_i - \frac{t_o + t_i}{2} \right) \sec \theta - 2t_f \dots \dots \dots (38)$$

Thus, the hydraulic diameter changes and varies the Reynolds number and thus ultimately changing the achievable overall heat transfer coefficient. The frictional factor and the Nusselt number correlation are the same to that of the helical coils without lean.

3.4. Geometry Implications

This section shows change in helical angle, Ψ and number of turns, N when heat exchanger length is varied. Figure 3-3 shows change in helical angle when heat exchanger length is varied for a fixed number of helical turns (in this case, $N = 1$).

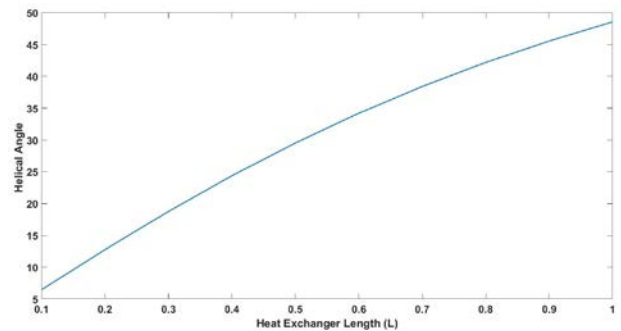


Figure 3.3: Helical Angle, Ψ vs Heat exchanger length, L for fixed $N = 1$

From the above figure, as heat exchanger length increases for a fixed N , the helical angle increases which in turn decrease the cross sectional area and perimeter as shown in equation (27) and (28). Figure 3-4 shows change in number of helical turns, N when heat exchanger length is varied for a fixed helical angle (in this case, $\Psi = 24.4^\circ$ (calculated for $N = 1$)).

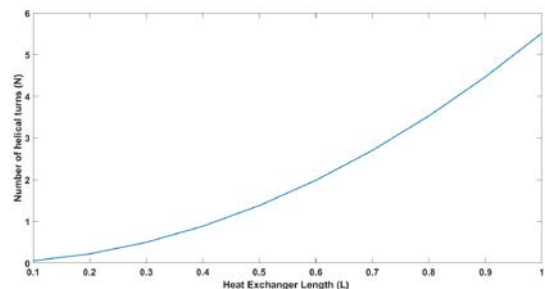


Figure 3.4: Number of helical turns, N vs Heat exchanger length, L for fixed $\Psi = 24.4^\circ$

In figure 3.4, as heat exchanger length increases for a fixed Ψ , number of helical turns increases too, but there is no change in cross sectional area and perimeter. However, the helical length increases as shown by equation (25).

Table 3.1 summarizes the important geometric parameters for the heat exchangers described in this section

Table 3.1: summary of important heat exchanger geometric parameters

parameter	$\theta = 0^\circ$	$\theta = 0^\circ$			$\theta = 45^\circ$		
	N=0	N=0.5	N=1	N=1.25	N=0.5	N=1	N=1.25
Ψ	90 ₀	42.2 ₀	24.4 ₀	19.9 ₀	42.2 ₀	24.4 ₀	19.9 ₀
L_{hlx}	1	1.49	2.42	2.93	1.49	2.42	2.93
A_{crs}	1	0.67	0.41	0.34	0.67	0.41	0.34
p	1	0.68	0.43	0.36	0.70	0.45	0.38
D_h	1	0.98	0.95	0.94	0.96	0.91	0.89

In Table 3.1, the straight channel case (N= 0, $\theta= 0^\circ$), the length, cross-sectional area, and wetted perimeter have been normalized to 1 as a baseline case. As the number of turns, N is increased, helical angle Ψ decreases, the helical length of the channel increases, the cross-sectional area and wetted perimeter decreases. When a lean angle, θ , is added to the helical cases, the length and cross-sectional area do not change, but the wetted perimeter increases, thus decreasing the hydraulic diameter. In helical case, there is an increase in length and thus the heat transfer area, which increases the heat transfer rate but also increases the pressure drop across the heat exchanger. Increasing the number of turns will result in higher heat transfer rate, but also a higher pressure drop.

IV. RESULTS

This section presents the results of a parametric study for the various heat exchanger geometries discussed above. The geometric constraints and flow conditions for the parametric study are summarized in Table 4.1.

Table 4.1: Heat exchanger design and performance parameters

Parameter Description	Value or Range	Type
-----------------------	----------------	------

Outer diameter, D_o	≤ 0.3 m	Constraint
Innermost diameter, D_s	≥ 0.2 m	Constraint
Length, L	≤ 0.4 m	Constraint
U_{ratio}	=1	Constraint
Pressure drop, Δp	$\leq 10\%$ of inlet pressure	Constraint
Hot fluid mass flow rate, \dot{m}_h	0.1 kg/s – 1 kg/s	Desired operating range
Cold fluid mass flow rate, \dot{m}_c	1 kg/s – 3kg/s	Desired operating range
Hot fluid inlet temperature, $T_{h,i}$	368k	Constraint
Hot fluid exit temperature, $T_{h,o}$	298k	Constraint
Cold fluid inlet temperature, $T_{c,i}$	278k	Constraint
Wall and fin thickness, t_o, t_i, t_f	1 mm	Constraint
Number of turns	-	Variable
Inner diameter, D_i	-	Variable
Fluids	Water, nitrogen	Constant

The constraints are set by the heat exchanger necessitated performance; variable parameters can be adjusted to achieve required performance.

The working fluids are water/water and water/nitrogen. The objective is to cool the incoming hot fluid from 368 K to 298 K using cold fluid which enters the heat exchanger at 278 K. Both fluids enter the heat exchanger with static pressure of 202 kPa. For the analysis the initial geometry are $D_o = 0.3$ m, $D_i = 0.287$ m, $D_s = 0.275$ m, $L = 0.4$ m, and the fin and wall thickness are all 1 mm. Diameters and wall thickness set the inner and outer channel heights.

The energy balance (Equation 1 and 2) and log mean temperature difference (Equation 4) are used to find the heat transfer rate or the power required to lower the temperature of the hot fluid and find the exit temperature of the cold fluid. As discussed in section II Equations (3) and (7) are used to find U_{req} and U_{ach} for different fluid mass flow rates. The next subsections present the performance results of the various heat exchanger geometries.

4.1. Straight annular heat exchanger without and with radial fins

Table 4.2 shows the U_{ratio} variation for different mass flow rates for straight heat exchanger without radial fins for sets of working fluid combination.

Table 4.2: Summary of analysis for straight heat exchanger without fins

	\dot{m}_h (kg/s)	\dot{m}_c (kg/s)	Q (kw)	T _{h,o} (K)	U _{req} (kw/m ² k)	U _{ach} (kw/m ² k)	U _{ratio}
Water – Water Heat Exchanger	1	1	303	351	45.71	0.537	0.01
	1	3	303	304	22.28	0.991	0.04
	0.1	1	30	286	1.925	0.132	0.07
	0.1	3	30	281	1.850	0.246	0.13
Nitrogen – Water Heat Exchanger	1	1	73	297	5.081	0.191	0.04
	1	3	73	285	4.603	0.455	0.10
	0.1	1	7	280	0.445	0.069	0.15
	0.1	3	7	279	0.441	0.091	0.20

In case of a straight heat exchanger without fins, U_{ratio} is less than 1 for different mass flow rate cases. This means the hot fluid is not cooled to the desired temperature for this design. To improve the U_{ratio} and to achieve the required drop in temperature for the hot fluid, fins are employed, which in turn increases the heat transfer area and thus the heat transfer rate. Table 4-3 summarizes changes in U_{ratio} when 8 fins are employed in both inner and outer channel Energy transfer rate, q and the exit temperature, $T_{h,o}$, of the cold fluid remains the same for different mass flow rate cases.

Table 4.3: U_{ratio} for straight annular heat exchanger with 8 radial fins in both the channels

\dot{m}_h (kg/s)	\dot{m}_c (kg/s)	U_{ratio}		L _{req} (m) to achieve $U_{ratio}=1$	
		Water	Nitrogen	Water	Nitrogen

		-water	water	-water	water
1	1	0.01	0.04	33.6	10.3
1	3	0.04	0.10	9.0	4.0
0.1	1	0.07	0.16	5.6	2.5
0.1	3	.014	0.21	2.9	1.9

In case of straight heat exchanger with fins, U_{ratio} nearly is the same when compared to the one without fins. There is a very small improvement in U_{ratio} , but not significant enough to cool down the hot fluid to the desired temperature. L_{req} is the heat exchanger length required to achieve $U_{ratio} = 1$. The frictional pressure loss for both sets of working fluids in a straight heat exchanger with and without radial fins is summarized in Table 4.4.

Table 4.4: Frictional pressure drop in a straight annular heat exchanger

Fluid	Mass flow rate (kg/s)	Δp for heat exchanger without fins (kpa)	Δp for heat exchanger with fins (kpa)	Δp for L _{req} (kpa)
Water – Water Heat exchanger				
Hot water	1	0.04	0.04	3.64
	0.1	0.001	0.001	0.01
Cold water	1	0.04	0.04	3.67
	3	0.33	0.36	2.61
Nitrogen – Water Heat exchanger				
Nitrogen	1	10.36	11.553	298
	0.1	0.15	0.16	0.78
Water	1	0.03	0.03	0.84
	3	0.34	0.36	1.74

Tables above summarizes the U_{ratio} and ΔP for a straight heat exchanger with and without fins, $U_{ratio} < 1$ in all the cases. There is increase in U_{ratio} for the design with fins when compared to that of design without fins, however the pressure loss increases too. A long heat exchanger might satisfy U_{ratio} and pressure drop constraints, however the design is not suitable if weight and compactness are considered. An improved design is needed to bring U_{ratio} to 1 and thus helically coiled heat exchanger is the next design tested.

4.2 Helical Annular Heat Exchanger with Radial Fins Having No Lean Angle

Helically coiled heat exchangers coiled offers advantages over conventional shell and straight tube heat exchangers

in terms of heat transfer rates. It accommodates a large heat transfer area in a small space, with high heat transfer coefficients. Tubes are wrapped around cylinder in a helical shape and number of turns or helical angle are varied which changes the length of the heat exchanger and ultimately the heat transfer area. Due to helical shape, a secondary flow (centrifugal force) is created within the channel and allows for better mixing and there is also an increase in the heat exchanger length leading to an increase in heat transfer area and thus a higher U_{ratio} . Increasing the number of turns or decreasing the helical angle increases the U_{ratio} . Table 4.5 showcases how U_{ratio} changes with increasing coil turns in a helical annular heat exchanger having radial fins with no lean.

Table 4.5: U_{ratio} for helical annular heat exchanger with radial fins no lean

\dot{m}_h (kg/s)	\dot{m}_c (kg/s)	U_{ratio}					
		Water –Water			Nitrogen-Water		
		N=0.5	N=1	N=1.25	N=0.5	N=1	N=1.25
1	1	0.03	0.10	0.15	0.16	0.44	0.63
1	3	0.11	0.29	0.42	0.25	0.61	0.87
0.1	1	0.30	0.65	0.85	0.40	1.16	1.64
0.1	3	0.42	0.79	1.00	0.48	1.25	1.77

Figure 4.1 illustrates how U_{ratio} and ΔP changes with increase in number of helical turns for water-water heat

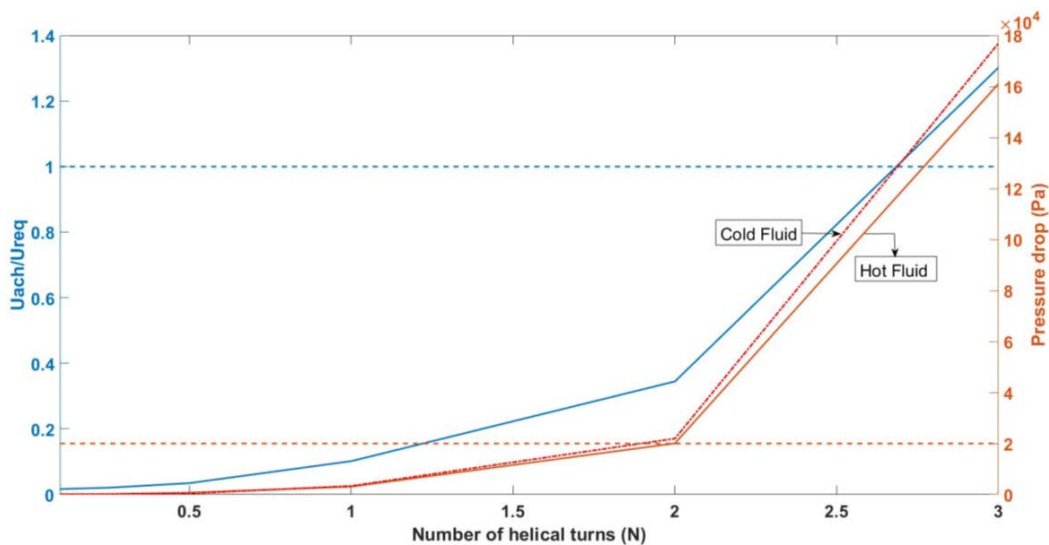


Figure 4.1: U_{ratio} and ΔP vs N for water-water heat exchanger

Table 4.5 shows U_{ratio} is high for helical heat exchanger when compared to a straight heat exchanger. Increase in turns leads to higher U_{ratio} . In a few cases U_{ratio} exceeds 1 and it means that the hot fluid is getting overcooled, i.e. beyond the desired temperature. When hot water-cold water is used as the working fluids, U_{ratio} equal to 1 is never attained for half turn or for a complete turn. In case of 1.25 turns, $U_{ratio}=1$ is achieved, thus cooling the hot water to the desired temperature. When nitrogen-water is used as the working fluid, 0.5, 1 and 1.25 turns does not meet the heat transfer goals. U_{ratio} is either less than or greater than 1 for all different mass flow rate combinations. $U_{ratio}=1$ can be achieved by varying the mass flow rates between the given range for hot and cold fluid. For example, with mass flow rates $\dot{m}_h = 0.385$ kg/s and $\dot{m}_c = 1$ kg/s and heat exchanger with 1.25 turns gives $U_{ratio}=1$ when nitrogen-water is used as working fluid.

As shown in table 4.3 the length required to bring in $U_{ratio}=1$ in case of $\dot{m}_h = 0.1$ kg/s and $\dot{m}_c = 3$ kg/s for straight counterflow water-water heat exchanger is 2.9 m. For the same mass flow rate combination in helical counterflow heat exchanger, for N corresponding to 1.25 turns, $U_{ratio}=1$ is achieved. The helical length corresponding to 1.25 turns is 1.17 m. The heat transfer goal has been met in a relatively shorter length which is 1.17 m, than the one calculated before which is 2.9 m. The reasoning for this interesting observation is, in the helical heat exchanger the cross sectional area decreases too in the process of increasing the number of turns. In decreasing the cross sectional area there is an increase in velocity and thus Reynolds number goes up, i.e. it becomes more turbulent. With the flow being more turbulent it helps in better mixing and with secondary flow formed, the heat exchange is quicker.

exchanger for a fixed mass flow rate, $\dot{m}_h = 1$ kg/s and $\dot{m}_c = 1$ kg/s.

In figure 4.1 the dotted blue line represents the heat transfer goal and the red dotted line represents the pressure drop threshold.

Due to build constraints, the fins in the heat exchanger are at a lean angle and the table 4.6 summarizes change in U_{ratio} with and without lean for $N = 1$.

4.3 Helical Annular Heat Exchanger with Radial Fins and Lean

Table 4.6: U_{ratio} comparison for helical annular heat exchanger with $\theta=0^\circ$ and $\theta=45^\circ$

\dot{m}_h (kg/s)	\dot{m}_c (kg/s)	Uratio			
		Water-Water		Nitrogen-Water	
		$\theta=0^\circ$	$\theta=45^\circ$	$\theta=0^\circ$	$\theta=45^\circ$
1	1	0.10	0.10	0.44	0.44
1	3	0.29	0.29	0.61	0.61
0.1	1	0.65	0.66	1.16	1.17
0.1	3	0.79	0.81	1.25	1.26

From the above table having a lean on the fins increases U_{ratio} marginally. The frictional pressure loss in a helical heat exchanger is summarized in table 4.7 for distinctive design cases.

Table 4.7: Frictional pressure drop in a helical annular heat exchanger for multiple N's

Fluids	Mass flow rate (kg/s)	Δp (kpa)			
		$N=0.5, \theta=0^\circ$	$N=1, \theta=0^\circ$	$N=1, \theta=45^\circ$	$N=1.25, \theta=45^\circ$
Water – Water Heat Exchanger					
Hot – water	1	0.74	3	3.14	5.23
	0.1	0.006	0.02	0.021	0.032
Cold – water	1	0.47	3.23	3.38	5.67
	3	4.47	27.28	28.53	47.81
Nitrogen – Water Heat Exchanger					
Nitrogen	1	1.85	748	782	1302
	0.1	2.91	11.78	12.32	20.51
Water	1	0.43	2.13	2.18	4
	3	4.43	27.53	28.8	48.25

Increase in number of turn's leads to an increase in heat exchanger helical length, decrease in cross sectional area and ultimately an increase in pressure loss. Pressure loss is

directly proportional to the length and inversely proportional to the square of the cross sectional area as shown in equation (13).

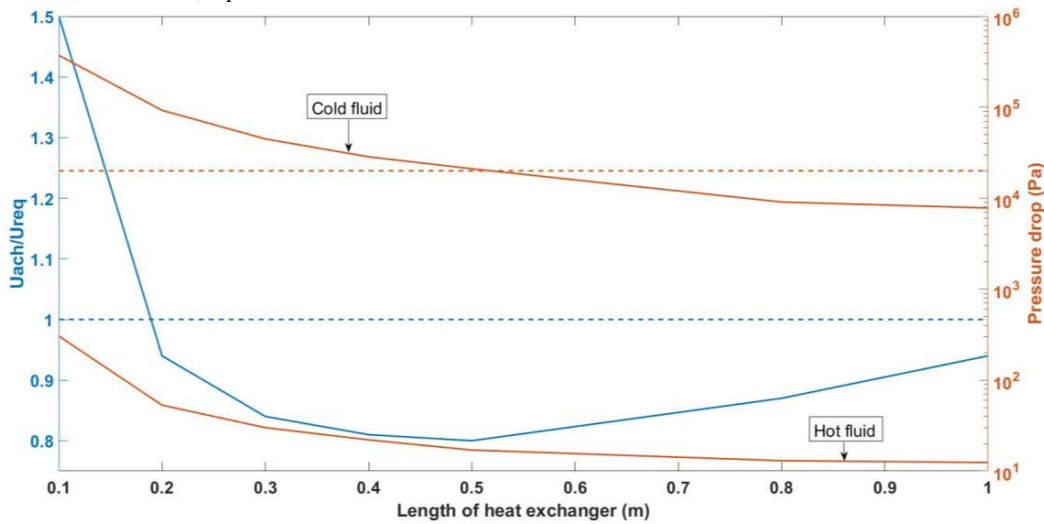


Figure 4.2: U_{ratio} and ΔP vs Heat exchanger length for water-water heat exchanger

Figure 4.2 shows changes in U_{ratio} and ΔP for increase in heat exchanger length for fixed number of helical turns $N = 1$, fixed heat exchanger diameter and fixed mass flow rate, $m_h = 0.1$ kg/s and $m_c = 3$ kg/s. There is a decrease in U_{ratio} till $L = 0.5$ m and then there is an increase after 0.5 m. The change in trend is due to change in flow regime,

turbulent to laminar. Figure 4-3 shows changes in U_{ratio} and ΔP for increase in heat exchanger diameter (D_o) for fixed number of helical turns $N = 1$, fixed heat exchanger length and fixed mass flow rate, $m_h = 0.1$ kg/s and $m_c = 3$ kg/s.

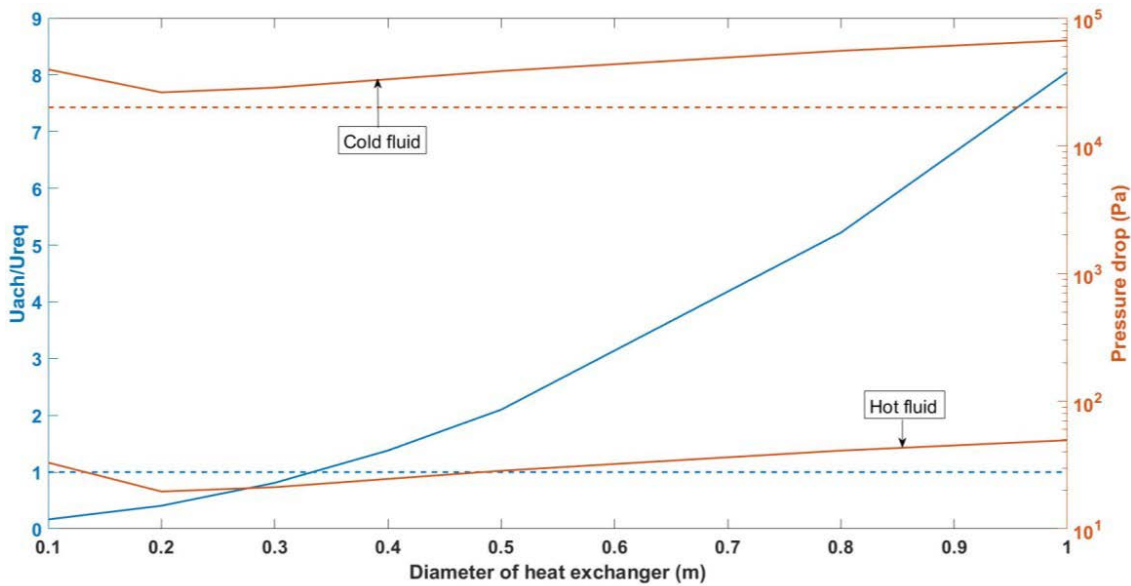


Figure 4.3: U_{ratio} and ΔP vs Heat exchanger diameter for water-water heat exchanger

As heat exchanger diameter increases U_{ratio} increases too. There is a decrease in pressure drop till diameter is 0.2 m and then pressure drop starts to increase after 0.2 m. Again the reason for change in trend is the flow regime change, i.e. turbulent to laminar.

V. PARAMETRIC STUDIES

In the previous section, an analytical model for various heat exchanger types were discussed and analyzed. Even

though helical heat exchangers are a compact design when compared to a standard straight tube in tube straight heat exchanger, this section investigates the possibility of designing a heat exchanger which is compact and lower in weight, but also achieves the required goal of a conventional design. Table 5.1 and 5.2 summarizes the optimized geometry and the resulting performance respectively for fixed mass flow rate of $m_h = 0.1$ kg/s and $m_c = 3$ kg/s.

Table 5.1: Design parameters for optimized geometry

Design	Diameters (m)	Number of fins	Number of helical turns	Length (m)
--------	---------------	----------------	-------------------------	------------

	D_o	D_i	D_s	Inner	Outer	Inner	Outer	
Water – Water Heat Exchanger								
1	0.3	0.269	0.247	8	8	2	2	0.4
2	0.3	0.269	0.247	11	10	1.75	1.75	0.3
3	0.26	0.221	0.209	11	10	2	2	0.4
1	0.26	0.221	0.209	4	4	1.125	1.125	0.1
Nitrogen – Water Heat Exchanger								
1	0.3	0.285	0.273	4	4	0.875	0.875	0.4
2	0.3	0.275	0.255	8	8	1.125	1.125	0.3
3	0.26	0.243	0.229	8	8	1.125	1.125	0.4
4	0.27	0.239	0.217	8	8	0.875	0.875	0.1

The design parameters summarized above have been based on the constraints and variables summarized in table 4.1.

All wall and fin thickness are 1 mm and fins are leaned at 45° in the above design models.

Table 5.2: Heat Exchanger performance for optimized geometry

Design	Uratio	Δp (kpa)		Volume (m3)	Mass (kg)
		Hot fluid	Cold fluid		
Water – Water Heat Exchanger					
1	1	0.019	13.42	0.0196	2.97
2	1	0.027	18.65	0.0071	2.27
3	1	0.101	7.59	0.0078	2.59
4	1	0.322	15.37	0.0141	0.61
Nitrogen – Water Heat Exchanger					
1	1	8.33	11.60	0.0212	2.96
2	1	20.13	7.53	0.0071	2.24
3	1	9.39	14.55	0.0078	2.60
4	1	15.13	20.76	0.0103	0.67

In case of water-water heat exchanger, design 1 is preferred if pressure loss is to be minimized or in other words higher efficiency. Design 4 is picked if compactness, i.e. weight and volume is important. Similarly, in case of Nitrogen-water design 1 is preferred if minimum pressure loss is wanted and design 4 if compactness is prioritized. There is tradeoff between pressure loss and compactness in all the above designs. For mass calculations aluminum having density of 2700 kg/m³ is used.

The different geometries shown in table 5.1 works only for $\dot{m}_h = 0.1$ kg/s and $\dot{m}_c = 3$ kg/s. When the same geometries are run at different flow rates within the range it does not meet the heat transfer goals and the pressure drop are not within the constraints too. Therefore, a better

optimized design is needed which works for the entire mass flow rate range.

Factors like thermal performance, pressure drop, heat exchanger weight and volume (compactness) are important in designing and optimizing a heat exchanger. Based on the vendor demands, one of these factors can be prioritized in designing.

5.1. Heat Transfer and Compactness prioritized for optimization

This section presents design and performance when heat transfer and compactness are prioritized. The design parameters for water-water and nitrogen-water heat exchanger are shown in table 5.3.

Table 5.3: Optimized design parameters when heat transfer and compactness are prioritized

Diameters (m)			Number of fins		Number of helical turns		Length (m)
D _o	D _i	D _s	Inner	Outer	Inner	Outer	
Water – Water Heat Exchanger							
0.3	0.277	0.255	8	8	4.5	45	0.3
Nitrogen – Water Heat Exchanger							
0.3	0.287	0.251	8	8	2.25	2.25	0.3

Table 5.4 summarizes changes in \dot{m}_{ratio} for the design parameters shown in table 5.3 for different mass flow rate combinations. The volume for both the heat exchangers is 0.0212 m³ and the mass for water-water is 2.24 kg and that of nitrogen-water is 2.27 kg.

Table 5.4: U_{ratio} for optimized design parameters when heat transfer and compactness are prioritized

\dot{m}_{h} (kg/s)	\dot{m}_{c} (kg/s)	U _{ratio}	
		Water – Water	Nitrogen- Water
1	1	1	1
1	3	2.96	1.19
0.1	1	3.95	2.09
0.1	3	4.47	2.15

As shown in the above table \dot{m}_{ratio} is greater than or equal to 1 for the entire mass flow rate range. For cases where \dot{m}_{ratio} is greater than 1, mass flow rate of the hot fluid should be increased or that of the cold fluid must be decreased, in order to bring \dot{m}_{ratio} to 1. However increasing or decreasing mass flow rates to satisfy heat transfer goals means going outside the mass flow rate

range. For example in case of water-water heat exchanger, the mass flow rate of the cold fluid must be decreased to 0.1 kg/s if the hot fluid flows at 0.1 kg/s to achieve $\dot{m}_{\text{ratio}} = 1$. Figure 5.1 and 5.2 illustrates change in \dot{m}_{ratio} for different mass flow rate combinations within the range for both water-water and nitrogen-water heat exchanger respectively.

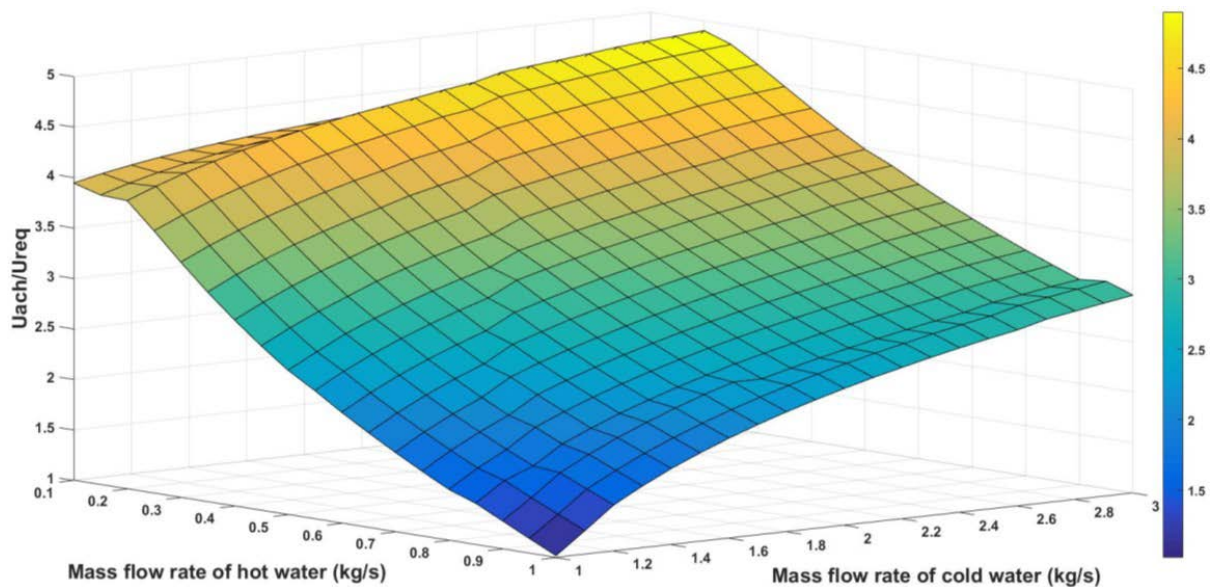


Figure 5.1: \dot{m}_{ratio} vs \dot{m}_{h} vs \dot{m}_{c} for water – water heat exchanger when heat transfer and compactness are prioritized

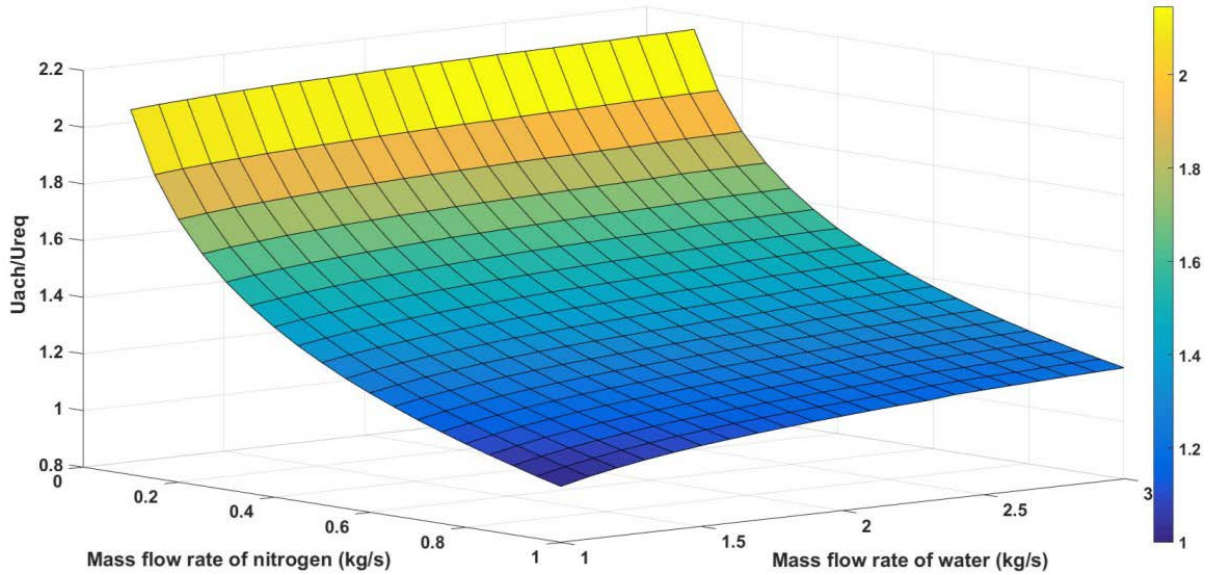


Figure 5.2: U_{ach}/U_{req} vs \dot{m}_w vs \dot{m}_n for nitrogen-water heat exchanger when heat transfer and compactness are prioritized

The biggest drawback with this design is the high pressure drop which accompanies with meeting heat transfer goals and compactness as shown in table 5.5. Pressure drop is beyond threshold for majority of the flow rate range.

Table 5.5: ΔP for Optimized design parameters when heat transfer and compactness are prioritized

Fluid	Mass flow rate (kg/s)	ΔP (kpa)
Water – Water Heat Exchanger		
Hot Water	1	87.20
	0.1	0.398
Cold Water	1	98.98
	3	834.43
Nitrogen – Water Heat Exchanger		
Nitrogen	1	640
	0.1	10.08
Water	1	60.22
	3	465.6

Figure 5.3 and 5.4 shows pressure drop variation with change in mass flow rates for the hot and cold fluid channel respectively for the water-water heat exchanger.

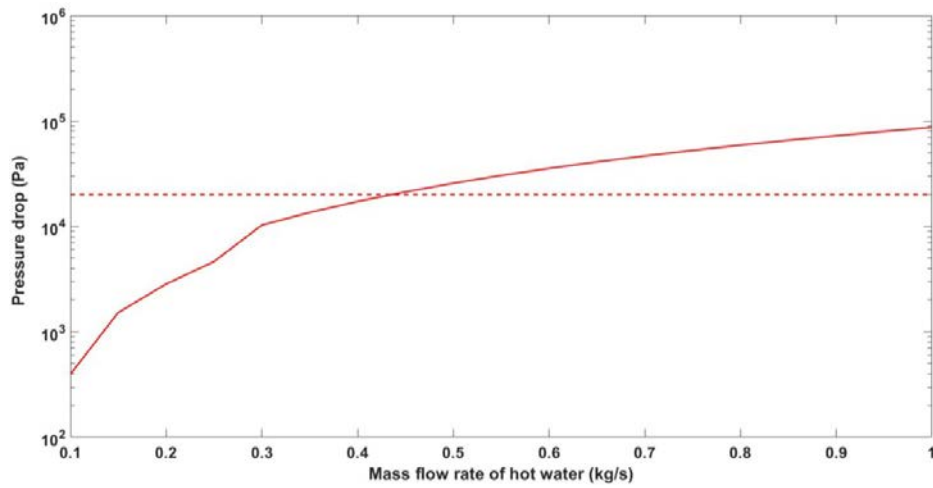


Figure 5.3: $\Delta \square$ vs \square for water - water heat exchanger when heat transfer and compactness are prioritized

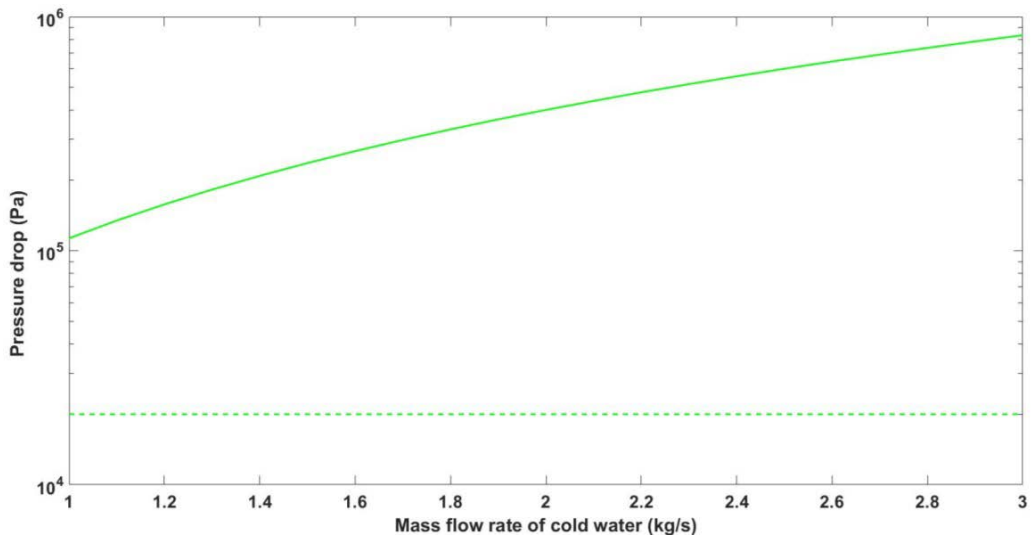


Figure 5.4: $\Delta \square$ vs \square for water - water heat exchanger when heat transfer and compactness are prioritized

Figure 5.5 and 5.6 shows pressure drop vs mass flow rates in hot and cold fluid channels respectively for the nitrogen-water heat exchanger.

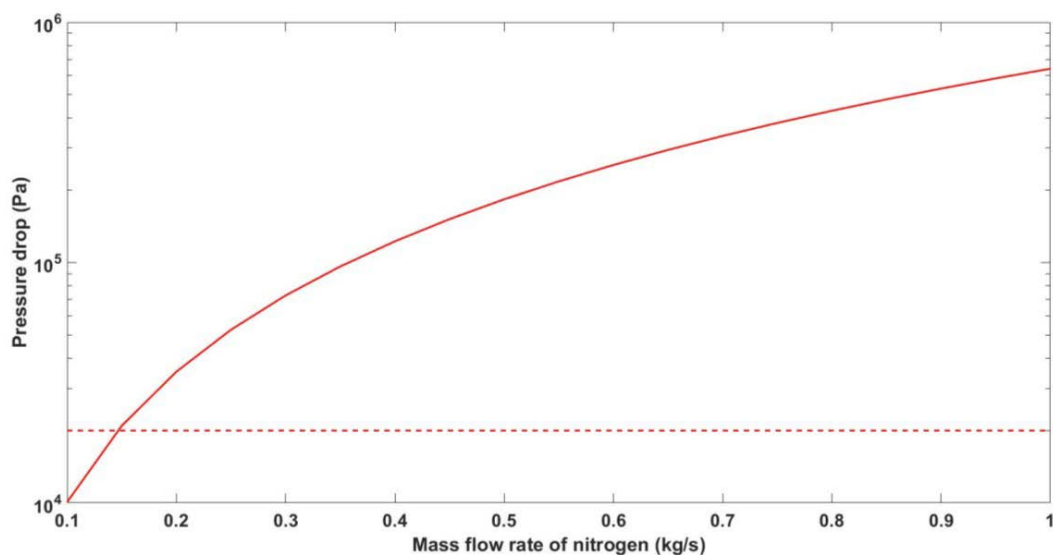


Figure 5.5: $\Delta \square$ vs \square for nitrogen - water heat exchanger when heat transfer and compactness are prioritized

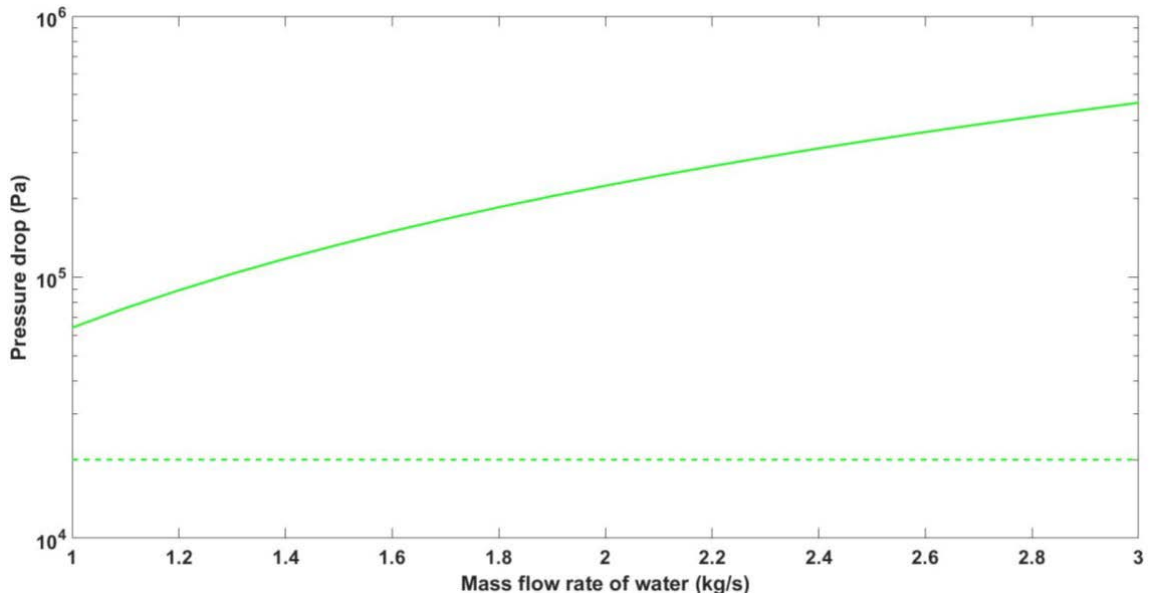


Figure 5.6: ΔP vs \dot{m} for nitrogen - water heat exchanger when heat transfer and compactness are prioritized

5.2 Pressure Drop and Compactness for optimization

This section presents a design and its performance when pressure drop and compactness are prioritized. The design

parameters for water-water and nitrogen-water heat exchanger are shown in table 5.6.

Table 5.6: Optimized design parameters when pressure drop and compactness are prioritized

Diameters (m)			Number of fins		Number of helical turns		Length (m)
D_o	D_i	D_s	Inner	Outer	Inner	Outer	
Water – Water Heat Exchanger							
0.26	0.229	0.215	8	8	1.75	1.75	0.26
Nitrogen – Water Heat Exchanger							
0.26	0.245	0.203	8	8	0.75	0.75	0.26

Figure 5.7 and 5.8 shows variation in pressure drop with change in mass flow rates for the hot and cold fluid channel respectively for the water-water heat exchanger.

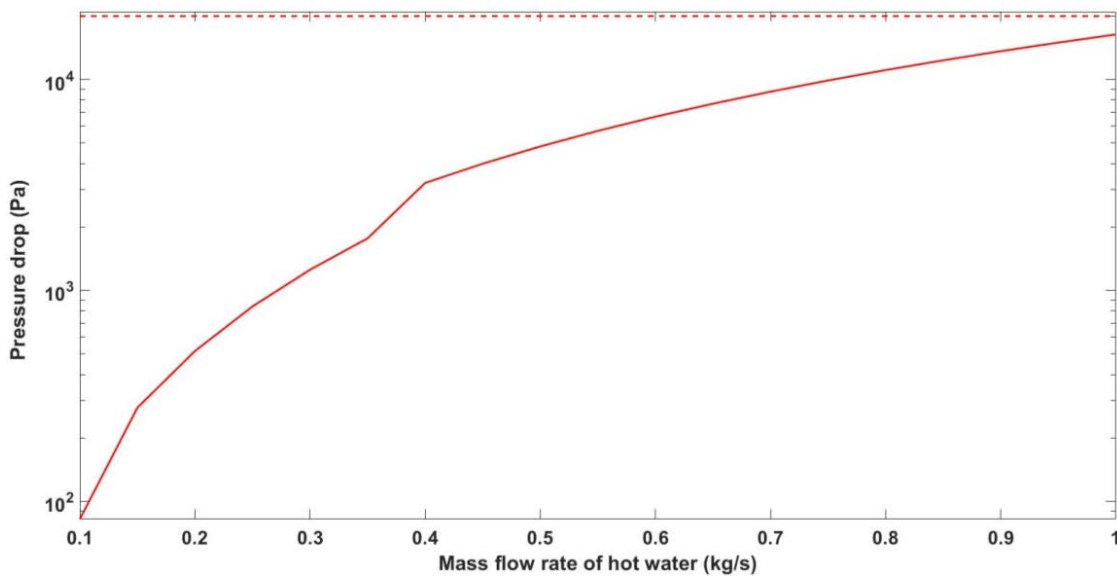


Figure 5.7: ΔP vs \dot{m} for water - water heat exchanger when pressure drop and compactness are prioritized

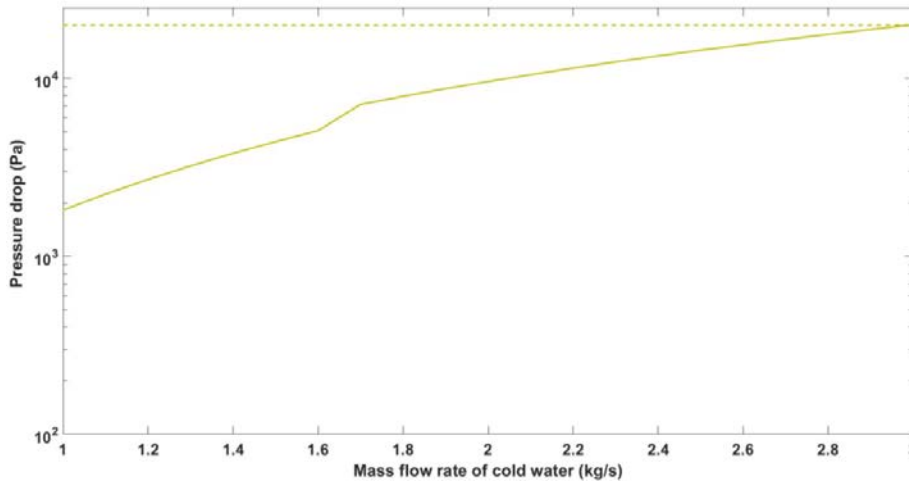


Figure 5.8: ΔP vs \dot{m}_c for water - water heat exchanger when pressure drop and compactness are prioritized

Table 5.7 summarizes the pressure drop for water-water and nitrogen-water heat exchangers and they are within the threshold for the given mass flow rate range.

Table 5.7: Δp for Optimized design parameters when pressure drop and compactness are prioritized

Fluid	Mass flow rate (kg/s)	ΔP (kpa)
Water – Water Heat Exchanger		
Hot Water	1	16.36
	0.1	0.083
Cold Water	1	2.38
	3	20
Nitrogen – Water Heat Exchanger		
Nitrogen	1	18.26
	0.1	0.288
Water	1	1.25
	3	15.28

Figure 5.9 and 5.10 shows pressure drop variation with change in mass flow rates for the hot and cold fluid channels respectively for the nitrogen-water heat exchanger.

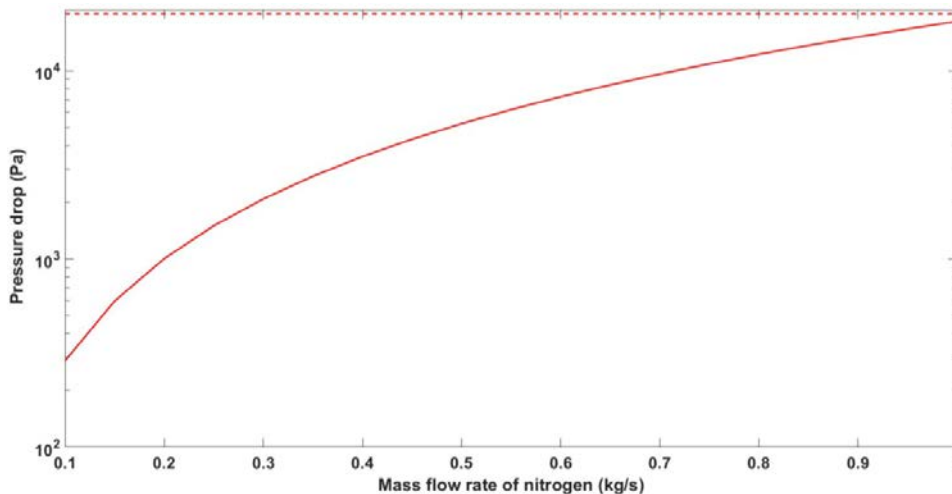


Figure 5.9: ΔT_{lm} vs \dot{m}_c for nitrogen - water heat exchanger when pressure drop and compactness are prioritized

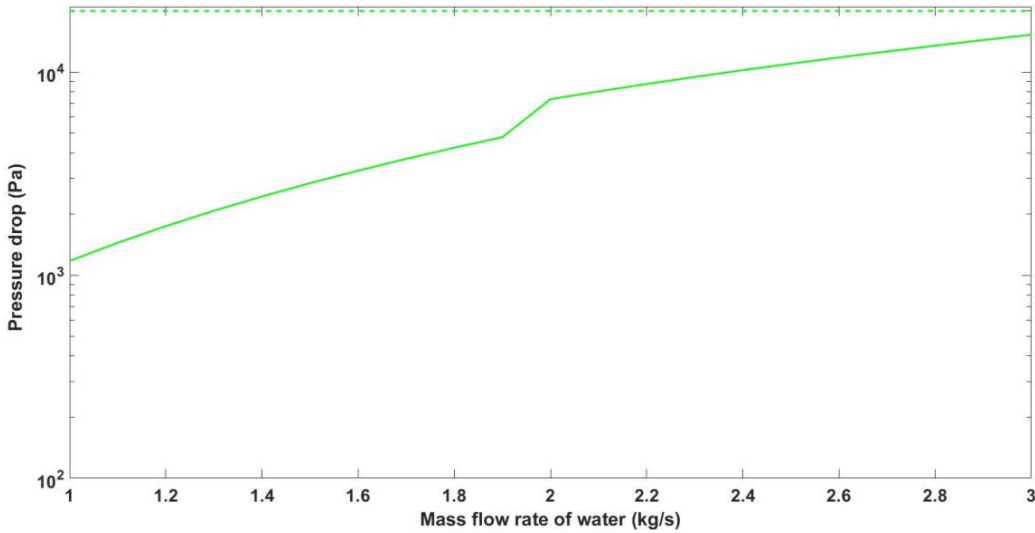


Figure 5.10: ΔT_{lm} vs \dot{m}_c for nitrogen - water heat exchanger when pressure drop and compactness are prioritized

Table 5.8 summarizes changes in U_{ratio} for the design parameters in table 5.6 for different mass flow rate combinations.

Table 5.8: U_{ratio} for Optimized design parameters when heat transfer and compactness are prioritized

\dot{m}_h (kg/s)	\dot{m}_c (kg/s)	U_{ratio}	
		Water – Water	Nitrogen- Water
1	1	0.12	0.12
1	3	0.40	0.14
0.1	1	0.78	0.25
0.1	3	1	0.26

In table 5.8 U_{ratio} is less than or equal to 1 for different mass flow rate combinations and is the main disadvantage when pressure drop and compactness are prioritized. U_{ratio} can be increased to 1 by either increasing the flow rate of cold fluid or by decreasing the hot fluid mass flow rate. The better option would be decreasing the mass

flow rate of hot fluid as it keeps the pressure drop within the constraints. Figure 5.11 and 5.12 illustrates change in U_{ratio} for different mass flow rate combinations within the mass flow rate range for both water-water and nitrogen-water heat exchanger respectively.

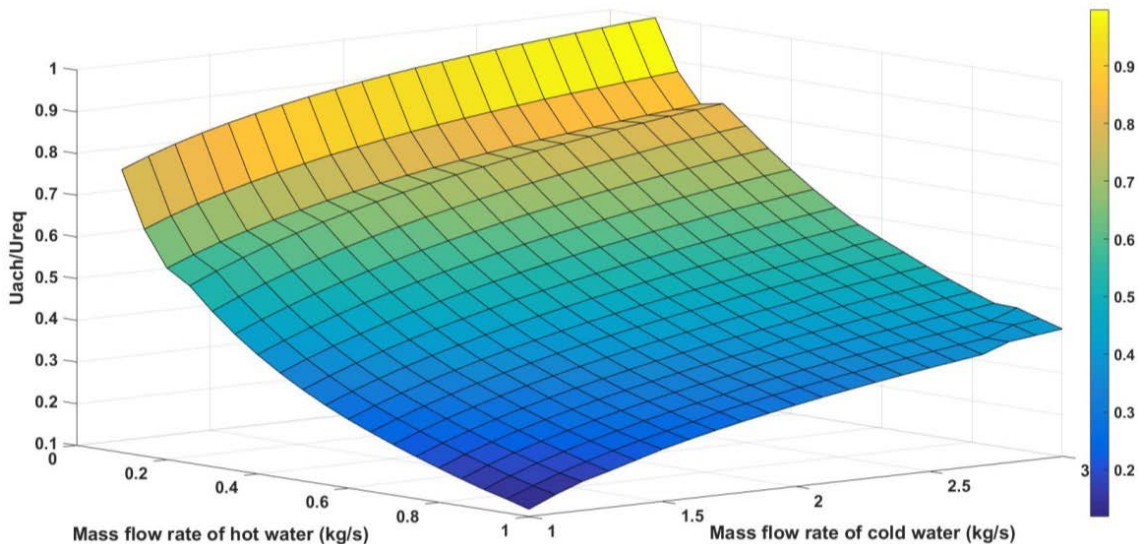


Figure 5.11: U_{ach}/U_{req} vs \dot{m}_w vs \dot{m}_n for water – water heat exchanger when Pressure drop and compactness are prioritized

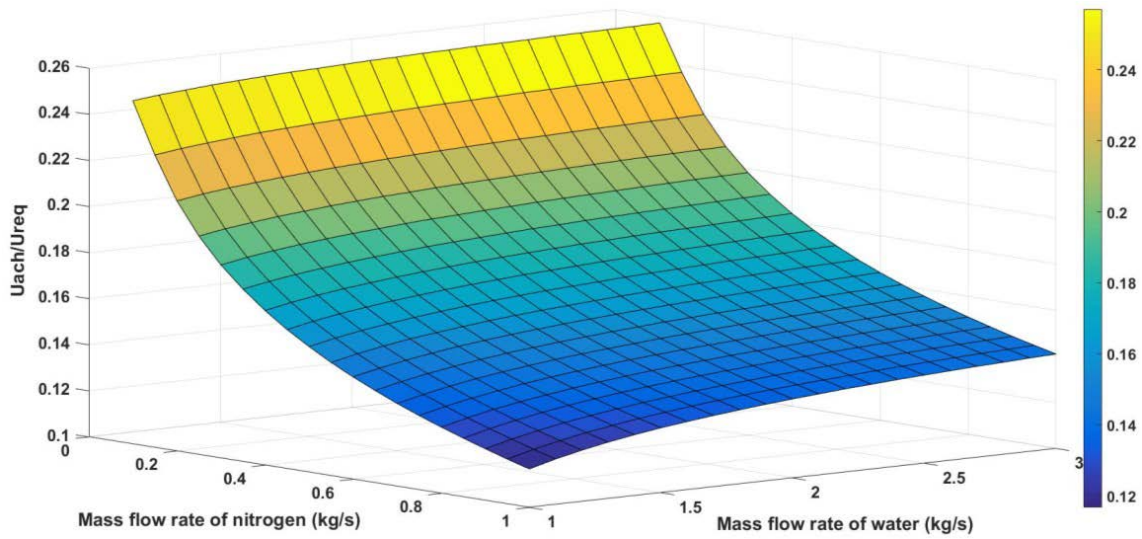


Figure 5.12: U_{ach}/U_{req} vs \dot{m}_w vs \dot{m}_n for nitrogen-water heat exchanger when Pressure drop and compactness are prioritized

The volume for both the heat exchangers is 0.016 m³ and the mass for water-water is 1.66 kg and that of nitrogen-water is 1.70 kg.

Table 5.9: Optimized design parameters when heat transfer and pressure drop are prioritized

Diameters (m)			Number of fins		Number of helical turns		Length (m)
D _o	D _i	D _s	Inner	Outer	Inner	Outer	
Water –Water Heat Exchanger							
0.75	0.723	0.709	8	8	2.5	2.5	0.75
Nitrogen – Water Heat Exchanger							
0.75	0.729	0.665	8	8	1.75	1.75	0.75

Table 5.10 summarizes changes in U_{ratio} for the design parameters shown in table 5.9 for different mass flow rate combinations.

Table 5.10: U_{ratio} for Optimized design parameters when heat transfer and pressure drop are prioritized

\dot{m}_w (kg/s)	\dot{m}_n (kg/s)	U_{ratio}	
		Water – Water	Nitrogen- Water
1	1	1	1
1	3	3.25	1.25
0.1	1	7.08	1.98
0.1	3	9.50	2.05

In table 5.10 too U_{ratio} is greater than or equal to 1 for the entire mass flow rate change. For cases where U_{ratio} is greater than 1, mass flow rate of the hot fluid should be increased or that of the cold fluid must be decreases, in order to bring U_{ratio} to 1. However increasing or

decreasing mass flow rates to satisfy heat transfer goals means going outside the mass flow rate range. Figure 5.13 and 5.14 illustrates change in U_{ratio} for different mass flow rate combinations within the range for both

water-water and nitrogen-water heat exchanger respectively.

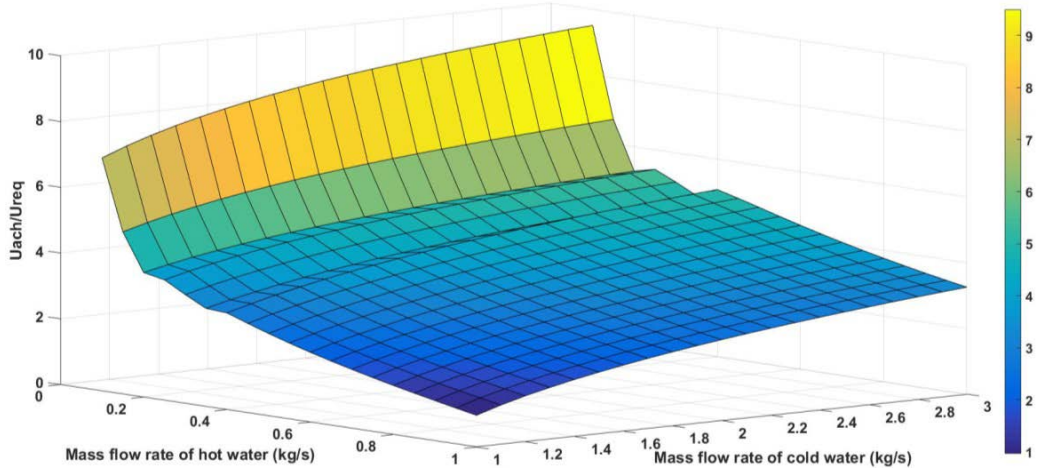


Figure 5.13: U_{ach}/U_{req} vs \dot{m}_h vs \dot{m}_c for water – water heat exchanger when heat transfer and pressure drop are prioritized

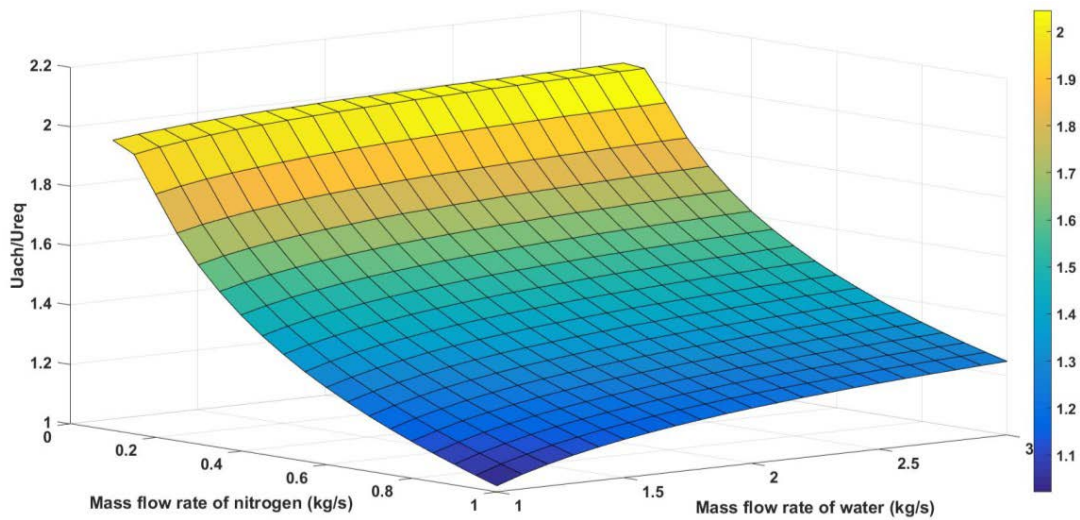


Figure 5.14: U_{ach}/U_{req} vs \dot{m}_n vs \dot{m}_w for nitrogen – water heat exchanger when heat transfer and pressure drop are prioritized

Figure 5.15 and 5.16 shows pressure drop vs mass flow rates for the hot and cold fluid channel respectively for the water-water heat exchanger.

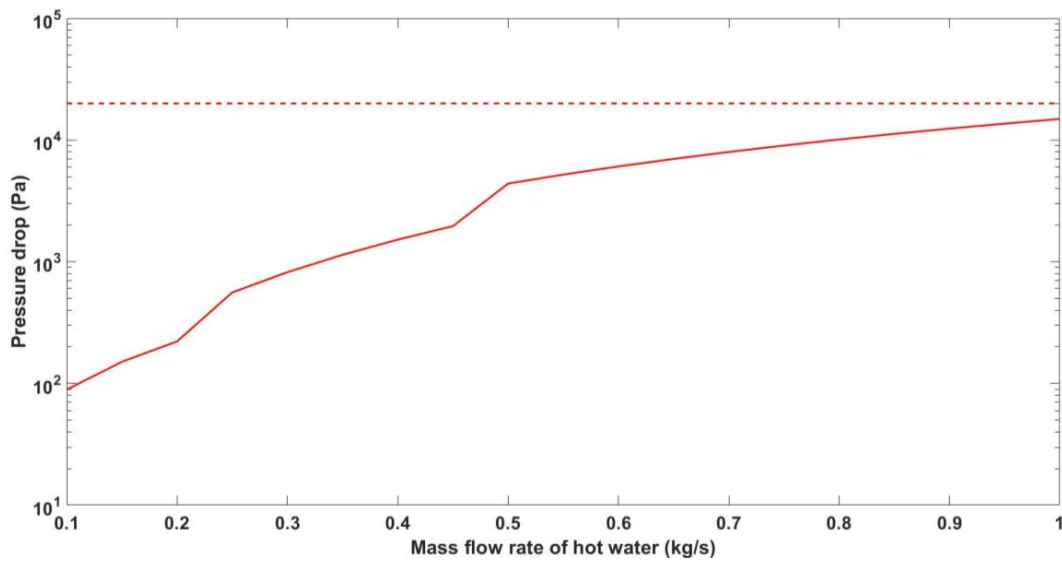


Figure 5.15: ΔP vs \dot{m}_h for water - water heat exchanger when heat transfer and pressure drop are prioritized

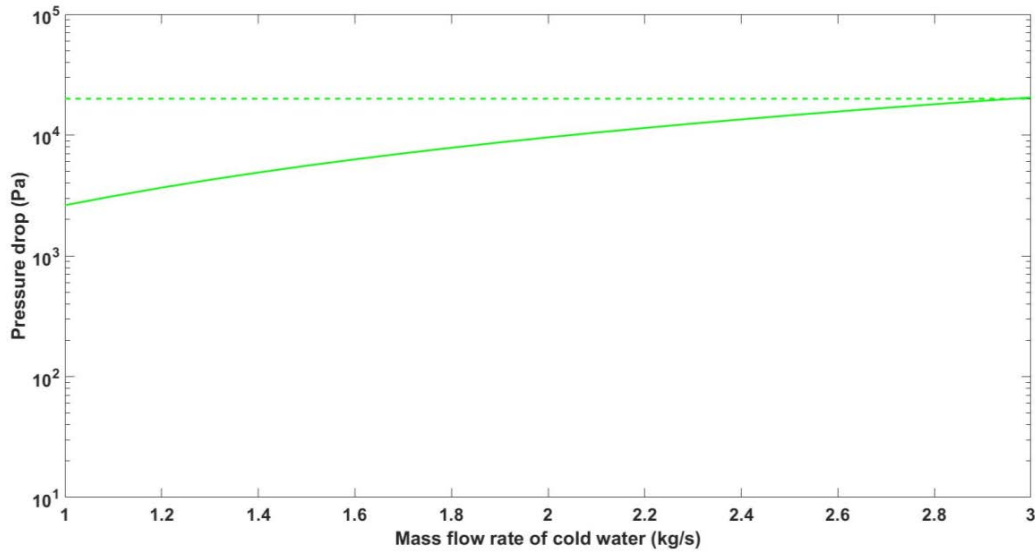


Figure 5.16: ΔP vs \dot{m}_c for water - water heat exchanger when heat transfer and pressure drop are prioritized

Table 5.11 summarizes the pressure drop for water-water and nitrogen-water heat exchangers and values are within the threshold for the given mass flow rate range

Table 5.11: Δp for Optimized design parameters when heat transfer and pressure drop are prioritized

Fluid	Mass flow rate (kg/s)	ΔP (kpa)
Water – Water Heat Exchanger		
Hot Water	1	14.91
	0.1	0.09
Cold Water	1	2.63
	3	20
Nitrogen – Water Heat Exchanger		
Nitrogen	1	18.5
	0.1	0.291
Water	1	1.08
	3	16.40

Figure 5.17 and 5.18 shows pressure drop vs mass flow rates for the hot and cold fluid channel respectively for the nitrogen-water heat exchanger.

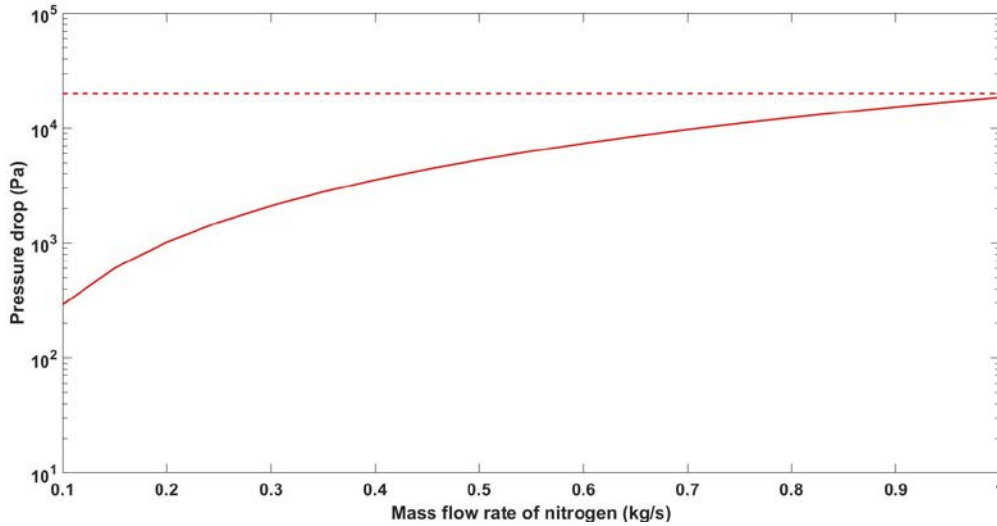


Figure 5.17: ΔP vs \dot{m} for nitrogen - water heat exchanger when heat transfer and pressure drop are prioritized

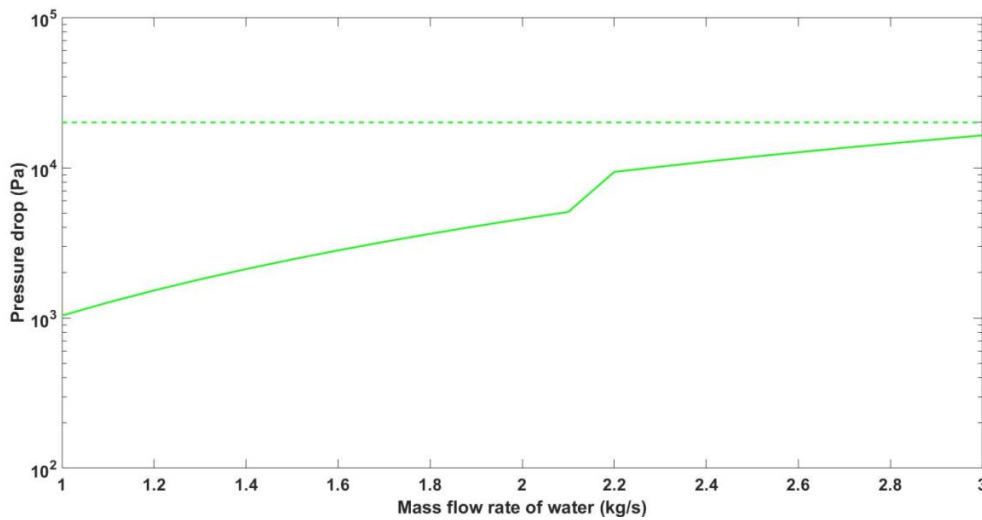


Figure 5.18: ΔP vs \dot{m} for nitrogen - water heat exchanger when heat transfer and pressure drop are prioritized

In this case the volume for both the heat exchangers is 0.331 m^3 and the mass for water-water is 14.2 kg and that of nitrogen-water is 14.3 kg .

To summarize a tradeoff between heat exchange, pressure loss and compactness is observed while designing an optimized model for given set of geometry constraints.

VI. CONCLUSIONS AND FUTURE WORK

This work explored the design and development of a novel high-performance, compact, counter flow heat exchanger design to utilize cold water to reduce the operating temperature of cryogenic nitrogen and hot water. New additive manufacturing approaches allow for 3D-printing of intricate design features that are not available using traditional approaches, however, additional constraints, such as a cantilever build angle to support the deposited metal material during the build.

Using a counter-flow and counter-helical design, an elevated level of heat exchange can be achieved in a compact volume, and the structure is robust enough to withstand the required operating pressures of the two fluids. Several designs were examined, based on a series of

given design constraints, and several candidate options were identified.

➤ Specific findings from this work are:

Helical heat exchangers offer significant advantage in heat exchange over straight tubular heat exchangers due to better mixing caused by the secondary flow in the helical coils. In case of helical heat exchangers there is an increase in heat transfer surface area for the same heat exchanger length and diameter.

Increase in number of helical turns increases the heat transfer area and thus the heat exchange. There is also decrease in cross sectional area which makes the flow more turbulent and with secondary flows being involved, heat exchange is better and improved. However, an increase in pressure drop is also observed in such cases which affect the efficiency of the heat exchanger

➤ Based on set of geometric constraints:

- If heat transfer and compactness are prioritized for optimization, pressure loss increases and goes beyond threshold

- If pressure drop and compactness are prioritized for optimization, heat transfer goals are not met
- If heat transfer and pressure drop are prioritized for optimization, then compactness in design are to be sacrificed
- In all above optimized designs, to bring $Uratio = 1$, it is required to go outside the mass flow rate range.

The same analysis and concept can be applied in designing heat exchangers for space applications with different fluids. Future work will include numerical and experimental investigations of the proposed highly compact and highly efficient heat exchanger design and an uncertainty/error analysis before experimenting the optimized design.

VII. REFERENCES

- [1]. T.J. Rennie. Numerical and experimental studies of a double-pipe helical heat exchanger. Ph.D. Dissertation, McGill University, Montreal, Canada, 2004.
- [2]. T.J. Rennie, G.S.V. Raghavan, Experimental studies of a double-pipe helical heat exchanger, *Exp. Therm. Fluid Sci.* 29 (2005) 919–924.
- [3]. V. Kumar, S. Saini, M. Sharma, K.D.P. Nigam, Pressure drop and heat transfer study in tube-in-tube helical heat exchanger, *Chem. Eng. Sci.* 61 (2006) 4403–4416.
- [4]. P. Naphon, Thermal performance and pressure drop of the helical-coil heat exchangers with and without crimped fins, *Int. Commun. Heat Mass Transfer* 34 (2007) 321–330.
- [5]. T.J. Rennie, D.G. Prabhanjan, Laminar parallel flow in a tube-in-tube helical heat exchanger, in: AIC Meeting, 2002.
- [6]. T.J. Rennie, G.S.V. Raghavan, Numerical studies of a double-pipe helical heat exchanger, *Appl. Therm. Eng.* 26 (2006) 1266–1273.
- [7]. V. Kumar, B. Faizee, M. Mridha, K.D.P. Nigam, Numerical studies of a tube in tube helically coiled heat exchanger, *Chem. Eng. Proc.* 47 (2008) 2287–2295.
- [8]. J.S. Jayakumara, S.M. Mahajania, J.C. Mandala, P.K. Vijayanb, R. Bhoia, Experimental and CFD estimation of heat transfer in helically coiled heat exchangers, *Chem. Eng. Res. Des.* 86 (2008) 221–232.
- [9]. Kays, W.M., and London, A.L., *Compact Heat Exchangers*. 3rd ed. 1984, McGraw-Hill: New York, NY
- [10]. Bergles, A.E., *Techniques to Enhance Heat Transfer*, in *Handbook of Heat Transfer*, W.M. Rohsenow, Hartnett, J.P., and Cho, Y.I., Editor. 1998, McGraw-Hill: New York, NY. p. 11.1-11.76
- [11]. Manglik, R.M., *Heat Transfer Enhancement*, in *Heat Transfer Handbook*, A. Bejan, and Kraus, A.D. Editor. 2003, Wiley: Hoboken, NJ, Ch. 14.
- [12]. Lee, S. P, Garimella, S.V. and Liu, D., Investigation of Heat Transfer in Rectangular Microchannels, *International Journal of Heat and Mass Transfer*, 2005. 48, p. 1688-1704.
- [13]. Harris, C. Despa, M., and Kelly, K., Design and Fabrication of a Cross Flow Micro heat Exchanger, *Journal of Microelectromechanical Systems*, 2000, 9(4), p. 502-508.
- [14]. Kandlikar, S., and Grande, W.J., Evolution of Microchannel Flow Passages-Thermohydraulic Performance and fabrication Technology, *Proceeding of ASME, International Mechanical Engineering Congress and Exposition*, 2006, IMECE2002-32043, ASME, New York, NY.
- [15]. Muley, A., Myott, B., Golecki, I., Borghese, J., Pohlman, M., White, S. and Strumpf, H., *Advanced Thermal Management Solutions for Aerospace Applications*, Sixth Biennial SAE Power Conference, 2004, Reno, NV.
- [16]. Boomsma, D., Poulikakos, D., and Zwick, F., Metal Foams as Compact High Performance Heat Exchanger, *Mechanics of Materials*, 2003, 35, p.1161-1176.
- [17]. Yu, Q. Straatman, A. G., and Thompson, B. E., Carbon-Foam Tubes in Air-Water Heat Exchangers, *Applied Thermal Engineering*, 2006, 26, p. 131-143
- [18]. Kim, S. Y., Paek, J. W. and Kang, B. H., Flow and Heat Transfer Correlations for Porous Fin a Plate - Fin Heat Exchanger, *ASME Transaction, Journal of Heat Transfer*, 2000, 122, p. 572-578.
- [19]. Fujii, M., Seshimo, Y., and Yamanaka, G., Heat Transfer and Pressure Drop of Perforated Surface Heat Exchanger with Passage Enlargement and Contraction. *International Journal of Heat and Mass Transfer*, 1988, 31(1): p. 135-142.
- [20]. R. L. Manlapaz, and S. W. Churchill, "Fully Developed Laminar Convection from a Helical Coil," *Chem. Eng. Commun.*, (9): 185-200, 1981.
- [21]. E. E Schmidt, "W~irmeibergang und Druckverlust in Rohrschlangen," *Chem. Ing. Tech.*, (39): 781-789, 1967.
- [22]. R. L. Manlapaz, and S. W. Churchill, "Fully Developed Laminar Flow in a Helically Coiled Tube of Finite Pitch," *Chem. Eng. Commun.*, (7): 57-78, 1980.
- [23]. <http://www.hydraulicspneumatics.com/200/TechZone/FluidPowerAcces/Article/False/6451/TechZone-FluidPowerAcces>
- [24]. Bahman Zohuri, Compact heat exchangers, Selection, Application, design and Evaluation, Springer, p. 21-30

[25]. http://www.heatric.com/typical_characteristics_of_PCHes.html.